Available online at www.sciencedirect.com
ScienceDirect
Catalysis Today 129 (2007) 43–49
CATALYSIS TODAY
www.elsevier.com/locate/cattod

Photocatalytic properties of surface modified platinised TiO_2: Effects of particle size and structural composition

M.C. Hidalgo *, M. Maicu, J.A. Navío, G. Colón

Instituto de Ciencia de Materiales de Sevilla, Centro mixto CSIC-Universidad de Sevilla, Américo Vespucio 49, 41092 Sevilla, Spain

Available online 3 August 2007

Abstract

Some parameters that may have an influence on the photocatalytic activity of TiO_2 modified by platinisation have been studied, including structural composition, source of TiO_2 or platinum-deposit size. A wide number of different TiO_2 was used for the study: commercial TiO_2 Degussa P25, Hombikat UV-100 and Rutile Aldrich as well as TiO_2 prepared by sol–gel method in our laboratory. Platinisation was performed in all cases over the different TiO_2 by photodeposition of platinum from hexachloroplatinic(IV) acid (H_2PtCl_6), depositing an amount of 0.5% Pt (weight total to TiO_2) and using isopropanol as reducting agent under N_2 atmosphere.

All samples were widely characterised: surface area and porosity, phase composition and crystallite size, UV–vis absorption properties, etc. The study of the platinum deposit sizes was attempted by transmission electron microscopy (TEM).

The enhancing or detrimental effect of the platinum deposits on the photocatalytic activity of the different TiO_2 for phenol oxidation was studied in correlation with the results of structural and surface characterisation.

Keywords: Pt/TiO_2; Commercial TiO_2; Platinisation; Rutile; Anatase; Photocatalysis; Phenol oxidation

1. Introduction

Doping of TiO_2, very often by deposition of noble metals as platinum, has been one of the strategies followed to increase the efficiency of photocatalysts [1–7]. The effect of platinisation on the photocatalytic activity of TiO_2 has been a controversial subject in the literature and reported experimental results have been sometimes contradictories [8,9]. The enhancement (or not) of the photocatalytic activity of TiO_2 by platinisation seems to depend highly on the substrate to be degraded [8,10] as well as on the properties and amount of deposited Pt [11,12].

Platinisation of TiO_2 continues to be a current topic in today photocatalysis research, as many publications on the subject in the last years show [2,4,8,12–18]. In any case, platinum influence on TiO_2 photocatalysis is not clear yet and needs further investigation.

For a better understanding of the factors that may have an influence on platinisation of TiO_2, we have studied the effect of several parameters on the photocatalytic properties of surface modified platinised TiO_2, such as structural composition and source of the TiO_2 and platinum particle size. For that, samples with unlike structural and physical properties were chosen as starting materials, i.e. TiO_2 with very different crystalline phase composition, surface areas, etc. were platinised with the same amount of Pt following the same platinisation method. Three commercial TiO_2, Degussa P25, Hombikat UV-100 and Rutile Aldrich, were used for the study as well as TiO_2 prepared by sol–gel method in our laboratory. The enhancing or detrimental effect of the platinum deposits on the photocatalytic activity of the different TiO_2 for phenol oxidation was studied in correlation with the results of structural and surface characterisation.

2. Experimental

2.1. Catalyst preparation

Platinisation was performed over three different commercial TiO_2 (Degussa P25, Sachtleben Hombikat UV-100 and Aldrich Rutile) and over a laboratory prepared TiO_2 obtained by a sol–gel method.

* Corresponding author. Tel.: +34 954489576; fax: +34 95 446 0665.
E-mail address: mchidalgo@icmse.csic.es (M.C. Hidalgo).

0920-5861/$ – see front matter © 2007 Elsevier B.V. All rights reserved.
doi:10.1016/j.cattod.2007.06.052

Laboratory prepared TiO_2 was obtained by the hydrolysis of titanium tetraisopropoxide (Aldrich, 97%) in isopropanol solution (1.6 M) by the addition of distilled water (volume ratio isopropanol/water 1:1). The precipitate then was filtered, dried at 110 °C overnight and calcined at 500 °C for 2 h.

Platinisation was performed over the TiO_2 samples (laboratory prepared TiO_2 calcined at 500 °C for 2 h and "as received" commercial samples) by photodeposition of platinum from hexachloroplatinic(IV) acid (H_2PtCl_6, Merck 40% Pt) following a modification of a method described elsewhere [1]. The nominal amount of Pt deposited was of 0.5% in weight in every case. This percentage was chosen because some previous works found amounts under 1 wt.% Pt as optima of metal loading for the photocatalytic properties of TiO_2 [1,2,9]. Suspensions of the different TiO_2 samples in distilled water were prepared (5 g TiO_2 L^{-1}) adding isopropanol to act as sacrificial agent (0.3 M final concentration) and the appropriate amount of H_2PtCl_6 under continuous nitrogen sparging. Photodepositions were performed by illumination of the suspensions for 6 h with a medium pressure mercury lamp (400 W) of photon flux ca. 2.6×10^{-7} Einstein s^{-1} L^{-1} in the region of wavelengths <400 nm. After recovering of the powders by filtration, the samples were dried at 110 °C overnight.

Portions of platinised samples were also calcined at 300 °C or 500 °C for 2 h and same calcination treatments were applied to the corresponding unmodified TiO_2 samples for comparative purposes.

Hereafter, samples will be denoted as P25, Hk, Rut or Tip (depending on the source of TiO_2: Degussa, Hombikat, Rutile Aldrich or laboratory prepared, respectively), followed by Pt (if the sample was platinised) and T3/T5 (if the sample was calcined at 300 °C or 500 °C, respectively).

2.2. Characterisation of the catalysts

The study of the samples by transmission electron microscopy (TEM) provided information about Pt deposits size and dispersion. TEM observations were performed using a Philips CM 200 instrument. The microscope was equipped with a top-entry holder and ion pumping system, operating at 200 kV and given a nominal structural resolution of 0.21 nm. The samples were dispersed in ethanol using an ultrasonicator and dropped on a carbon grid.

Absorption properties of the samples were studied by UV–vis spectroscopy. UV–vis spectra were measured on a Varian spectrometer model Cary 100 equipped with an integrating sphere and using $BaSO_4$ as reference. All the spectra were recorded in diffuse reflectance mode and transformed to a magnitude proportional to the extinction coefficient through the Kubelka-Munk function, $F(R\infty)$.

Crystalline phase composition and degree of crystallinity of the samples were estimated by X-ray diffraction (XRD). XRD patterns were obtained on a Siemens D-501 diffractometer with Ni filter and graphite monochromator using Cu Kα radiation. Crystallite sizes of the different phases were estimated from the line broadening of the corresponding X-ray diffraction peaks by using the Scherrer equation [19]. Peaks were fitted by using a Voigt function, defined as a convolution between a Gaussian and a Lorentzian function.

BET surface area and porosity measurements were carried out by N_2 adsorption at 77 K using a Micromeritics ASAP 2010 instrument.

2.3. Photocatalytic runs

The photocatalytic activity of the samples was tested for phenol oxidation, chosen as model reaction. Suspensions of the samples (1 g L^{-1}) in phenol solution (50 ppm) were placed in a batch reactor (200 mL) and illuminated through a UV-transparent Plexiglas® top window (threshold absorption at 250 nm) by an Osram Ultra-Vitalux lamp (300 W) with sun-like radiation spectrum and a main line in the UVA range at 365 nm. The intensity of the incident UVA light on the solution was measured with a PMA 2200 UVA photometer (Solar Light Co.) being ca. 95 W m^{-2}. Magnetic stirring and oxygen flow were used to produce a homogeneous suspension of the catalyst in the solution. Prior illumination, catalyst-substrate equilibration was allowed by stirring the suspension 20 min in the dark. The evolution of the phenol concentration was measured by UV–vis spectrometry following its 270 nm characteristic band.

Blank experiments were performed in the dark as well as with illumination and no catalyst, without observable change in the initial concentration of phenol in both cases.

The "enhancement factor", E-factor, defined as the rate of a photoprocess over a sample with platinum divided by the rate of the same photoprocess over the sample without platinum [11], was calculated for all the platinised samples for phenol oxidation.

3. Results

3.1. Characterisation of platinised and non-platinised samples

Three commercial TiO_2 were used for platinisation: Degussa P25 (non-porous, mixture of phases anatase–rutile), Hombikat UV-100 (low crystallinity, high surface area, anatase phase) and Rutile Aldrich (low surface area, rutile phase). The laboratory prepared TiO_2 calcined at 500 °C for 2 h presented mainly anatase phase and relatively high crystallinity, with a BET surface area (46 m^2 g^{-1}) comparable to the one of Degussa P25 (51 m^2 g^{-1}). A summary of characterisation results of platinised and non-platinised samples is presented in Table 1a. As it can be seen, platinisation did not significantly change the surface areas, crystalline phase compositions or the primary particle sizes of the samples. Only the surface area of TiO_2 Hombikat decreased slightly after the photodeposition, nevertheless keeping a relatively high value (260 m^2 g^{-1}). XRD of the platinised samples (pattern not shown) displayed no Pt peaks, since metal sites are expected to be below the detection limit of X-ray analysis.

In Fig. 1, selected TEM micrographs are shown. The study of the platinised samples by TEM gives an indication of Pt

Table 1a
Summary of characterisation results for the different photocatalyst

Catalyst	Notation	Phase composition (%)[a]	Primary TiO_2 particle size (nm)[b]	S_{BET} ($m^2\ g^{-1}$)
Degussa P25	P25	80% A, 20% R	22 (anatase)	51
Pt/Degussa P25	P25Pt	80% A, 20% R	22 (anatase)	51
Hombikat UV-100	Hk	100% A	9 (anatase)	280
Pt/Hombikat UV-100	HkPt	100% A	9 (anatase)	260
Rutile Aldrich	Rut	8% A, 92% R	43 (rutile)	13
Pt/Rutile Aldrich	RutPt	8% A, 92% R	43 (rutile)	14
Sol–gel TiO_2 (500 °C, 2 h)	Tip	ca. 100% A, B (traces)	17 (anatase)	46
Pt/sol–gel TiO_2 (500 °C, 2 h)	TipPt	ca. 100% A, B (traces)	18 (anatase)	48

[a] A: anatase, R: rutile, B: brookite.
[b] Calculated by the Scherrer equation.

deposits size and dispersion. As it can be observed, photodeposited platinum-islands were spherical and well dispersed on the TiO_2 surface of all samples, having diameters within different ranges depending on the sample (Table 2). Thus, the smallest deposits could be found on the surface of samples TipPt and RutPt, with Pt-particle sizes mainly within 1.5 and 3 nm, and the largest Pt-particles belonged to sample HkPt, with particles mainly within 6 and 8 nm.

According to Zhang et al. [20] and Vorontsov et al. [21], under the conditions of photodeposition used in this work (pH 4.5, long deposition time, isopropanol as sacrificial agent in relatively high concentration, absence of oxygen) platinum should be deposited mainly in the form of Pt^0. The valence state of platinum deposits can also have an important influence on the photocatalytic activity of platinised samples, being Pt^0 the form of Pt reported to lead to highest photoactivities [12,20,21].

The absorption properties of the samples were studied by diffuse reflectance UV–vis spectroscopy (spectra not shown for the sake of brevity). Band-gaps were calculated by using the

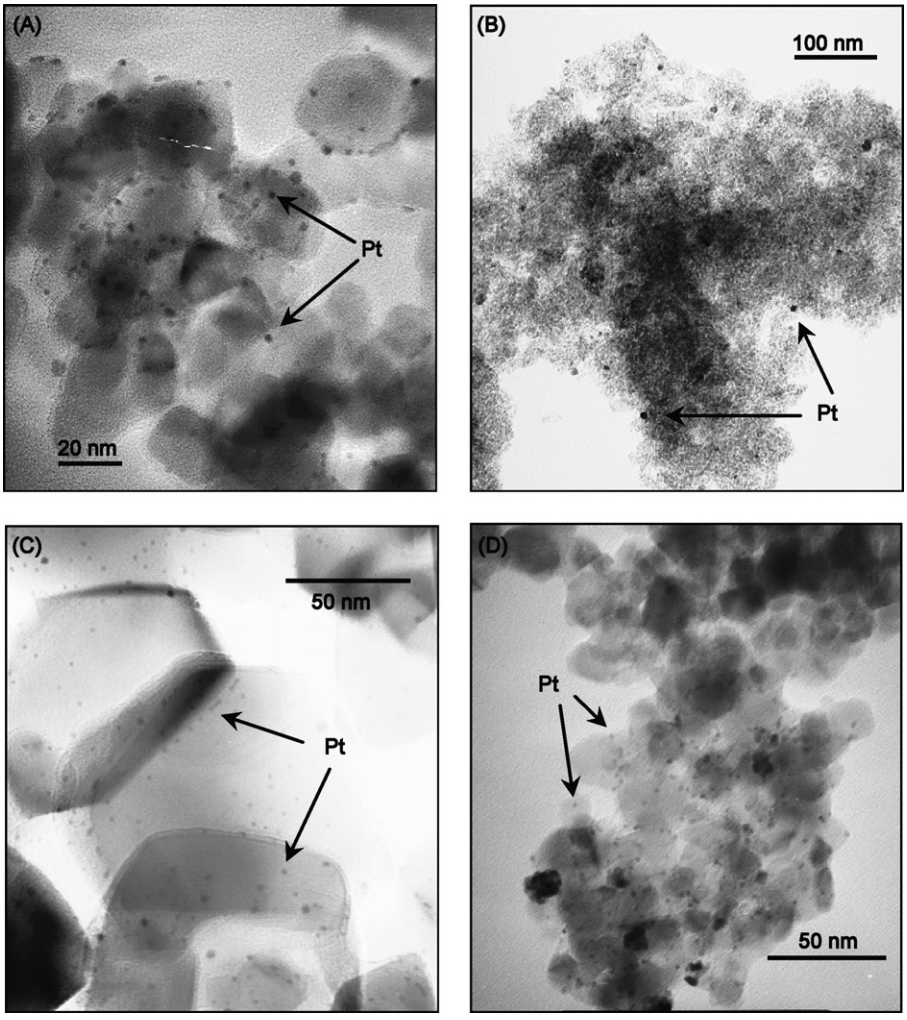

Fig. 1. Selected TEM photographs of platinised samples over Degussa P25 (A), Hombikat UV-100 (B), Rutile Aldrich (C) and sol–gel TiO_2 (D).

Kubelka-Munk functions according to the method proposed by Tandom and Gupta [22]. All samples with anatase as main crystalline phase had band-gap values around 3.5 eV. Rutile Aldrich presented a smaller value of band-gap, 3.2 eV, which is characteristic of TiO_2 rutile. On the other hand, comparison between the diffuse reflectance spectra of platinised and non-platinised samples showed no differences in the UV range. Due to their dark grey colour, platinised samples showed a stronger absorption respect to unmodified samples throughout the visible range.

3.2. Effects of calcination temperature after platinisation

Portions of the platinised samples were calcined at 300 and 500 °C for 2 h after photodeposition. The respective non-platinised samples were also calcined at the same temperatures for comparison purposes.

A summary of characterisation results for these calcined samples is shown in Table 1b. No significant differences in crystalline phase composition or primary TiO_2 crystallite size could be observed between calcined and non-calcined samples. Only anatase crystallite size for Hk increased slightly with the calcination temperature. BET surface area of P25 as well as of Tip samples (platinised and non-platinised) decreased slightly with calcination. The decrease of BET surface area in sample HkPt was more noticeable, from 260 to 141 $m^2\ g^{-1}$ (300 °C) and 85 $m^2\ g^{-1}$ (500 °C). Non-platinised sample Hk presented the same tendency (Table 1b.). Rutile samples showed not significant changes in surface area after calcination treatments.

Series TipPt, TipPtT3 and TipPtT5 were also studied by TEM. Estimated ranges of Pt deposit sizes are shown in Table 2. Sizes of Pt particles increased with calcination temperature and consequently number of particles decreased too. Number and size of the Pt-deposits can have a large influence on the photoactivity of the samples.

Table 2
Range of platinum deposit sizes estimated by TEM observations for the different platinised catalysts

Sample notation	Estimated range of Pt particle sizes (nm)	Number of Pt particles considered for the estimation[a]
P25Pt	4–6	ca. 45
HkPt	6–8	ca. 25
RutPt	1.5–3	ca. 125
TipPt	2–3	ca. 100
TipPtT3	2.5–4	ca. 125
TipPtT5	4–8	ca. 25

[a] Approximately same number of TEM photographs was considered for each sample (less particles were found per surface unit as the average Pt particle size increased).

3.3. Photocatalytic activity for phenol degradation

The photocatalytic activity of the samples was tested in the reaction of photo-oxidation of phenol. Initial degradation rates and *enhancement*-factors for platinised samples are presented in Table 3. Rates for phenol degradation of selected samples are also shown in Fig. 2. An improvement in the photocatalytic activity of the samples after platinisation can be observed for all set of samples except for P25, where the activity decreased with platinisation. This improvement is larger in rutile Aldrich, presenting the highest E-factor of all pairs of samples.

Regarding calcination temperatures after platinisation, E-factors showed a similar trend for all series of samples (with E-factor >1), as it can be seen in Fig. 3: the improvement of platinisation was larger for samples calcined at 300 °C, decreasing for samples calcined at 500 °C. E-factors were calculated comparing phenol oxidation rates of calcined platinised samples with also calcined non-platinised samples.

In absolute values, the most active sample was the laboratory prepared TiO_2 platinised and calcined at 300 °C for 2 h

Table 1b
Summary of characterisation results for the different calcined samples

Catalyst	Notation	Phase composition (%)[a]	Primary TiO_2 particle size (nm)[b]	S_{BET} ($m^2\ g^{-1}$)
Degussa P25 300 °C, 2 h	P25T3	80% A, 20% R	22 (anatase)	n.m.
Pt/Degussa P25 300 °C, 2 h	P25PtT3	80% A, 20% R	22 (anatase)	49
Degussa P25 500 °C, 2 h	P25T5	80% A, 20% R	22 (anatase)	n.m.
Pt/Degussa P25 500 °C, 2 h	P25T5	80% A, 20% R	22 (anatase)	44
Hombikat 300 °C, 2 h	HkT3	100% A	12 (anatase)	151
Pt/Hombikat 300 °C, 2 h	HkPtT3	100% A	12 (anatase)	141
Hombikat 500 °C, 2 h	HkT5	100% A	17 (anatase)	84
Pt/Hombikat 500 °C, 2 h	HkPtT5	100% A	17 (anatase)	85
Rutile Aldrich 300 °C, 2 h	RutT3	8% A, 92% R	44 (rutile)	12
Pt/Rutile Aldrich 300 °C, 2 h	RutPtT3	8% A, 92% R	43 (rutile)	12
Rutile Aldrich 500 °C, 2 h	RutT5	8% A, 92% R	43 (rutile)	12
Pt/Rutile Aldrich 500 °C, 2 h	RutPtT5	7% A, 93% R	44 (rutile)	13
Sol–gel TiO_2 (500 °C, 2 h) 300 °C, 2 h	TipT3	ca. 100% A, B (traces)	20 (anatase)	37
Pt/Sol–gel TiO_2 (500 °C, 2 h) 300 °C, 2 h	TipPtT3	ca. 100% A, B (traces)	18 (anatase)	46
Sol–gel TiO_2 (500 °C, 2 h) 500 °C, 2 h	TipT5	ca. 100% A, B (traces)	22 (anatase)	39
Pt/sol–gel TiO_2 (500 °C, 2 h) 500 °C, 2 h	TipPtT5	ca. 100% A, B (traces)	21 (anatase)	44

n.m.: not measured
[a] A: anatase, R: rutile, B: brookite.
[b] Calculated by the Scherrer equation.

Table 3
Results of photocatalytic activity for phenol degradation

Sample notation	Initial reaction rate $\times 10^{-3}$ (mg s^{-1} L^{-1})	E-factor
P25	11.94	–
P25Pt	8.71	0.73
P25T3	13.69	–
P25PtT3	8.84	0.65
P25T5	10.43	–
P25PtT5	8.00	0.77
Hk	5.29	–
HkPt	8.30	1.57
HkT3	5.56	–
HkPtT3	12.93	2.33
HkT5	9.47	–
HkPtT5	12.16	1.28
Rut	3.47	–
RutPt	10.23	2.95
RutT3	2.82	–
RutPtT3	9.08	3.22
RutT5	2.13	–
RutPtT5	4.53	2.13
Tip	9.88	–
TipPt	11.38	1.15
TipT3	7.01	–
TipPtT3	17.45	2.49
TipT5	9.23	–
TipPtT5	9.09	0.98

(TipPtT3), being notably more active than Degussa P25 (Fig. 4). It is worth to notice that degradation profiles of phenol for platinised samples did not show any important deceleration at prolonged illumination times, as it can be noticed in Fig. 4. In any case total degradation of phenol was reached within 1–3 h, suggesting that no resistant intermediate is formed for phenol oxidation over platinised samples, as reported by Siemon et al. for EDTA degradation where Pt became detrimental in the last stages of the reaction [10].

4. Discussion

TiO_2 photocatalysts with different structural and surface characteristics were modified by platinisation and their photocatalytic properties were evaluated for phenol photo-oxidation. Platinisation provided no significant change in surface area, composition of crystalline phases or TiO_2 primary

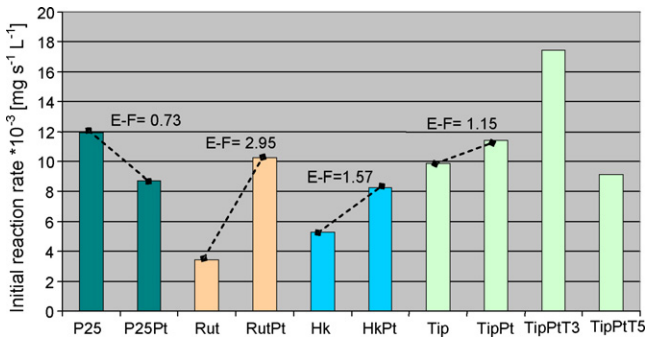

Fig. 2. Initial reaction rate for phenol photo-oxidation over the different photocatalysts. $[Phenol]_0 = 50$ mg L^{-1}, $V = 0.2$ L, [Catalyst] = 1 g L^{-1}, $I = 95$ W m^{-2}.

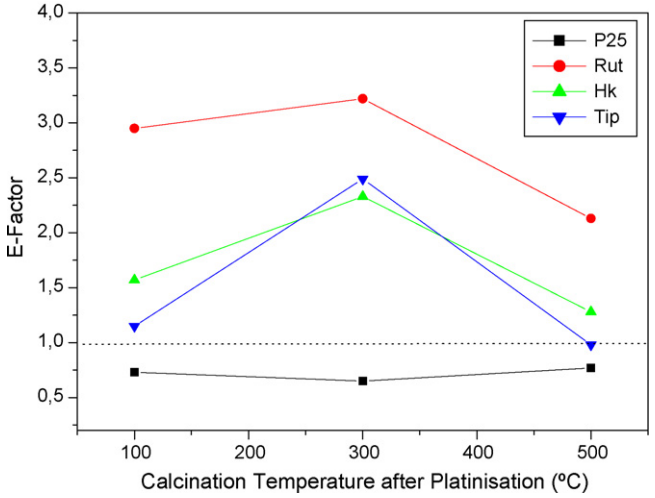

Fig. 3. Enhancement-factor (E-factor) of the different platinised samples with the calcination temperature for the reaction of photooxidation of phenol. $[Phenol]_0 = 50$ mg L^{-1}, $V = 0.2$ L, [Catalyst] = 1 g L^{-1}, $I = 95$ W m^{-2}.

particle size (Table 1a), and therefore differences in photo-activities are not due to these effects.

It is nowadays accepted that noble metal nanoparticles as platinum deposited on the TiO_2 surface are effective traps for photogenerated electrons due to the formation of a Schottky barrier at the metal-semiconductor contact. These electrons can improve the rate of reduction of oxygen (cathodic half-reaction in the photocatalytic process) and reduce the probability of electron–hole recombination [10–12]. According to our results, for Hk, Tip and Rut samples, composed mainly by an only phase, Pt deposits could be beneficial by reducing the overpotential of electron transfer to adsorbed oxygen and all the subsequent oxidative reactions. For the two-phases P25 sample, Pt could not further increase the efficiency of charge separation by the capture of electrons and reduction of oxygen, since the junction between the two phases anatase and rutile already provides an optimum path for electron–hole separation: holes are concentrated in rutile and electrons are left in anatase particles [9,15] before migration to the corresponding particle surface, and probably for this reason platinisation did not

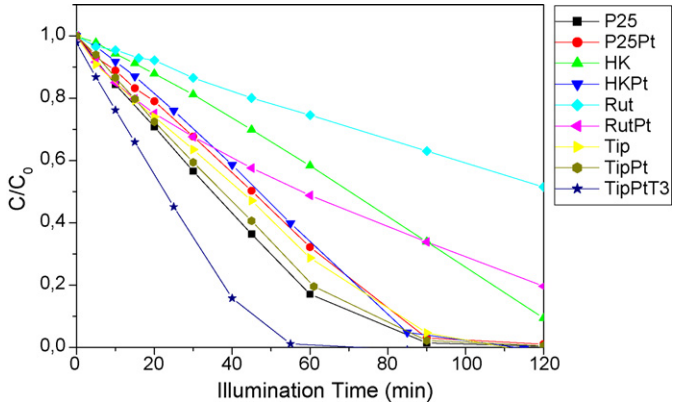

Fig. 4. Profiles of phenol degradation over the different unmodified and platinised photocatalysts with the illumination time. $[Phenol]_0 = 50$ mg L^{-1}, $V = 0.2$ L, [Catalyst] = 1 g L^{-1}, $I = 95$ W m^{-2}.

produce an improvement in the photoactivity for phenol photo-oxidation. Furthermore, even a slightly detrimental effect of platinum was observed for this sample, maybe due to the reduction of TiO_2 available active sites by the blockage of platinum deposits. Thus, the type of TiO_2 becomes also crucial to the improvement or not of the photoefficiency by platinisation.

The *enhancement*-factor of Rutile Aldrich was found to be the highest of all the series (see Table 3, Fig. 3). It is known that the mobility of electrons in rutile is two order of magnitude lower than in anatase, resulting in a higher electron–hole recombination rate. It has also been reported that photo-generated electrons in rutile cannot be efficiently transferred to adsorbed oxygen due to an insufficient concentration of active oxygen vacancies on rutile surface [23]. Both detrimental effects will be largely avoided by having platinum deposits acting as electron sinks, and this would explain the high improvement of efficiency reached by platinisation of Rut sample, which is nearly 100% rutile, compared to the other samples formed by anatase phase.

It is worth noticing the relatively high activity shown by the non-platinised Rut sample for phenol photo-oxidation (Fig. 2), being not so much lower than that shown by Hk, especially if one takes into account the large difference in surface area between both samples ($13\ m^2\ g^{-1}$ versus $280\ m^2\ g^{-1}$) and consequently the number of active sites available. This result is interesting as it has been generally accepted that the photocatalytic activity of rutile is substantially lower than that of anatase [24,25].

In any case, it is also remarkable the high photocatalytic activity showed by the sol–gel TiO_2 samples (with and without platinum) and the platinised-rutile sample; activities comparable or even much higher than that of Degussa P25, which could be important in the searching of better alternatives to this commercial TiO_2.

Regarding calcination treatments after platinisation of the samples, it could be observed that the highest improvements of photoactivity were reached by the samples calcined at 300 °C, decreasing for samples calcined at 500 °C (Fig. 3). This observation could not be explained by changes in surface area, phase composition or absorption properties of platinum during the calcination treatments (see Section 3.2). On the contrary, with the calcination temperature the range of Pt deposit sizes became larger (Table 2). This could indicate that within the same sample there is an optimum size of deposited particle for the photoefficiency improvement effect, and afterward larger particles become detrimental for the photoefficiency of the samples. These findings are partially in disagreement with results reported by Lee and Choi [12], where platinum particle sizes had not a direct influence on the photocatalytic activity of platinised TiO_2 samples. A deeper study on this respect is currently under way.

5. Conclusions

In this work the effect of several parameters on the photocatalytic properties of surface modified platinised TiO_2, such as structural composition and source of the TiO_2 and platinum particle size, have been studied. Different TiO_2 were used for the study: commercial TiO_2 Degussa P25, Hombikat UV-100 and Rutile Aldrich as well as TiO_2 prepared by sol–gel method.

Platinisation did not significantly change surface area, crystalline phase composition or primary particle size of the samples. Photodeposited platinum particles were well dispersed on the TiO_2 surface for all samples, having different diameters depending on the sample. All samples showed improved photocatalytic activity for phenol oxidation with the platinisation, with the exception of TiO_2 Degussa P25. In this sample, platinum acting as electron sink could not further increase the efficiency of charge separation since this separation would be already optimised by the junction between the two phases anatase and rutile, where holes move into rutile and electrons are left in anatase particles. The E-factor of Rutile Aldrich sample was found to be the highest of all series. Mobility of electrons in rutile is two orders of magnitude lower than in anatase, therefore platinum deposits acting as electron sinks would avoid largely the high electron–hole recombination occurring in the original unmodified rutile and consequently would increase the photoefficiency of the platinised sample. These results confirmed that not only phase composition of TiO_2 but the way these phases are interconnected will have an important influence on the improvement or detrimental effect of platinisation on the photocatalytic activity of TiO_2.

An optimum of calcination temperature for the platinised samples was found at 300 °C. At this temperature, platinum deposits showed larger diameters than those in uncalcined samples. At higher calcination temperature, E-factors decreased again, at the same time that platinum particles became larger, suggesting an optimum size of Pt-deposits for photocatalytic activity within the same series of sample.

Acknowledgements

This research was financed by the Spanish Ministerio de Educación y Ciencia (project ref. CTQ2004-05734-C02-02). Partial financial support by the Junta de Andalucía (P.A.I. group reference FQM181) is also acknowledged. M.C.H. thanks the Spanish Ministerio de Educación y Ciencia (Ramón y Cajal Programme N.2003/116) for financial support.

References

[1] D. Hufschmidt, D. Bahnemann, J.J. Testa, C.A. Emilio, M.I. Litter, J. Photochem. Photobiol. A 148 (2002) 223.
[2] S. Sakthivel, M.V. Shankar, M. Palanichamy, B. Arabindoo, D. Bahnemann, V. Murugesan, Water Res. 38 (2004) 3001.
[3] G. Colón, M. Maicu, M.C. Hidalgo, J.A. Navío, Appl. Catal., B 67 (2006) 41.
[4] Y.Z. Yang, C.-H. Chang, H. Idriss, Appl. Catal., B 67 (2006) 217.
[5] G. Colón, M.C. Hidalgo, M. Macías, J.A. Navío, Appl. Catal. A 259 (2004) 235.
[6] F. Fresno, C. Guillard, J.M. Coronado, J.M. Chovelon, D. Tudela, J. Soria, J.M. Herrmann, J. Photochem. Photobiol. A 173 (2005) 15.
[7] V. Iliev, D. Tomova, R. Todorovska, D. Oliver, L. Petrov, D. Todorovsky, M. Uzunova-Bujnova, Appl. Catal. A 313 (2006) 115.

[8] F. Denny, J. Scott, K. Chiang, W.Y. Teoh, R. Amal, J. Mol. Catal. A 263 (2006) 93.
[9] B. Sun, A.V. Vorontsov, P.G. Smirniotis, Langmuir 19 (2003) 3151.
[10] U. Siemon, D. Bahnemann, J.J. Testa, D. Rodríguez, M.I. Litter, N. Bruno, J. Photochem. Photobiol. A 148 (2002) 247.
[11] S.K. Lee, A. Mills, Platinum Metals Rev. 47 (2003) 61.
[12] J. Lee, W. Choi, J. Phys. Chem. B 109 (2005) 7399.
[13] A. Patsoura, D.I. Kondarides, X.E. Verykios, Appl. Catal. B 64 (2006) 171.
[14] B. Sun, P.G. Smirniotis, P. Boolchand, Langmuir 21 (2005) 11397.
[15] C.A. Emilio, M.I. Litter, M. Kunst, M. Bouchard, C. Colbeau-Justin, Langmuir 22 (2006) 3606.
[16] P. Panagiotopoulou, A. Christodoulakis, D.I. Kondarides, S. Boghosian, J. Catal. 240 (2006) 114.
[17] Y.Z. Yang, C.H. Chang, H. Idriss, Appl. Catal. B 67 (2006) 217.
[18] S. Yin, T. Sato, J. Photochem. Photobiol. A 169 (2005) 89.
[19] B.D. Cullity, Elements of X-Ray diffraction, Addison Wesley Publishing Company Inc, 1978,, p. 284.
[20] F. Zhang, J. Chen, X. Zhang, W. Gao, R. Jin, N. Guan, Y. Li, Langmuir 20 (2004) 9329.
[21] A.V. Vorontsov, E.N. Savinov, J. Zhensheng, J. Photochem. Photobiol. A 125 (1999) 113.
[22] S.P. Tandom, J.P. Gupta, Phys. Stat. Sol. 38 (1970) 363.
[23] E. Wahlstrom, E.K. Vestergaard, R. Schaub, A. Ronnau, M. Vestergaard, E. Laegsgaard, I. Stensgaard, F. Besenbacher, Science 303 (2004) 511.
[24] T. Ohno, K. Sarukawa, M. Matsumura, J. Phys. Chem. B 105 (2001) 2417.
[25] M.C. Hidalgo, G. Colón, J.A. Navío, J. Photochem. Photobiol. A 148 (2002) 341.